

Supporting information

Efficient blue, green and red iridium(III) complexes with noncovalently-linked pyrazole/pyrazolide rings for organic light-emitting diodes

Jun-Jian Lu,^{1,2#} Xiao Liang,^{1#} Xu-Feng Luo,¹ Zheng-Guang Wu^{1*} and You-Xuan Zheng^{1*}

¹State Key Laboratory of Coordination Chemistry, Collaborative Innovation Center of Advanced Microstructures, Jiangsu Key Laboratory of Advanced Organic Materials, School of Chemistry and Chemical Engineering, Nanjing University, Nanjing 210093, P. R. China, E-mail: wuzhengguang_zy@163.com, yxzheng@nju.edu.cn.

²Department of Chemistry and Materials Science, Hunan University of Humanities, Science and Technology, Loudi 417000, P. R. China, E-mail: lujunjian2001@126.com

Lu and Liang have same contributions to this paper.

General information

¹H NMR spectra were measured on Bruker AM 400 spectrometer. The high resolution electrospray ionization mass spectra (HR ESI-MS) were recorded on an Bruker MTQ III q-TOF. Thermal analysis were measured on PerkinElmer Pyris 1 DSC. UV-vis absorption and photoluminescence spectra were measured on Shimadzu UV-3100 and Hitachi F-4600 spectrophotometer at room temperature, respectively. Cyclic voltammetry measurements were carried out using chi600 electrochemical workstation with Fc⁺/Fc as the standard at the rate of 0.1 V s⁻¹, using CH₂Cl₂ and tetramethylammonium hexafluorophosphate as the solvent and electrolyte salt, respectively. The decay lifetimes were measured with a HORIBA Scientific 3-D fluorescence spectrometer. High-resolution mass spectra were recorded on a MICROTOF-Q III instrument.

1,2-Diazole (98%), 2-(2,4-difluorophenyl)pyridine (98%), 2-(4-methylphenyl)pyridine (95%), 4-chloroquinazoline (95%), iridium trichloride (98%), sodium carbonate (99%), 2-ethoxyethanol (99%), methanol (99.9%), acetonitrile (99.9%) were purchased from Energy Chemical and Shanghai Medical Company (China), respectively. All other reagents were used as received from commercial sources, unless otherwise stated. The materials for OLED fabrication (HATCN (hexaazatriphenylenehexacarbonitrile, 99.8%), TAPC (1,1-bis(4-(di-*p*-tolylamino)phenyl)cyclohexane, 99.8%), 2,6-DCzPPy (2,6-bis(3-(carbazol-9-yl)phenyl)pyridine, 99.8%), TmPyPB (1,3,5-tri(*m*-pyrid-3-yl-phenyl)benzene, 99.8%, LiF (99.8%) and Al (99.99%)) were purchased from Luminescence Technology Corp. (Taiwan, China).

X-ray crystallography

X-ray crystallographic measurements of the single crystals were carried out on Bruker APEX-II CCD diffractometer (Bruker Daltonic Inc.) using monochromated Mo K α radiation ($\lambda = 0.71073 \text{ \AA}$) at room temperature. Cell parameters were retrieved using SMART software and refined using *S*AINT¹ program in order to reduce the highly redundant data sets. Data were collected using a narrow-frame method with scan width of 0.30° in ω and an exposure time of 5 s per frame. Absorption corrections were applied using *S*ADABS² supplied by Bruker. The structures were solved by direct methods and refined by full-matrix least-squares on F^2 using the program *S*HELXS-2014.³ The positions of metal atoms and their first coordination spheres were located from direct-Emaps, other non-hydrogen atoms were found in alternating difference Fourier syntheses and least-squares refinement cycles and during the final cycles refined anisotropically. Hydrogen atoms were placed in calculated position and refined as riding atoms with a uniform value of U_{iso} .

OLEDs fabrication and measurement

All OLEDs were fabricated on the pre-patterned ITO-coated glass substrate with a sheet resistance of $15 \Omega \text{ sq}^{-1}$. The approximate pressure during the vacuum deposition of the device layer stack was about $1.0\sim 4.0\times 10^{-4}$ Pa. The deposition rate for organic compounds (HATCN, TAPC, 2,6-DCzPPy, TmPyPB) is $1\text{-}2 \text{ \AA s}^{-1}$. The phosphors and host 2,6-DCzPPy were co-evaporated to form emitting layer from different sources. The cathode consisting of LiF/Al was deposited by evaporation of LiF with a deposition rate of 0.1 \AA s^{-1} and then by evaporation of Al metal with a rate of 3 \AA s^{-1} . All layers were deposited consecutively in the device. The effective area of the emitting diode is 0.1 cm^2 . The characteristics of the devices were measured with a computer controlled KEITHLEY 2400 source meter with a calibrated silicon diode in air without device encapsulation. On the basis of the uncorrected PL and EL spectra, the Commission Internationale de l'Eclairage (CIE) coordinates were calculated using a test program of the Spectra Scan PR650 spectrophotometer.

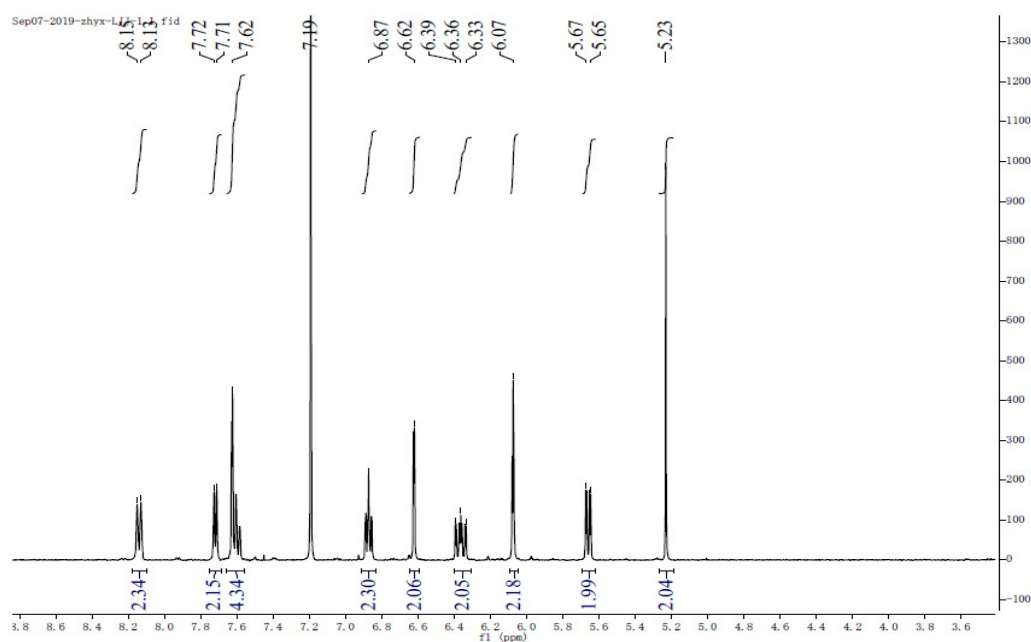


Fig. S1 The ^1H NMR spectrum of B-Ir1-H.

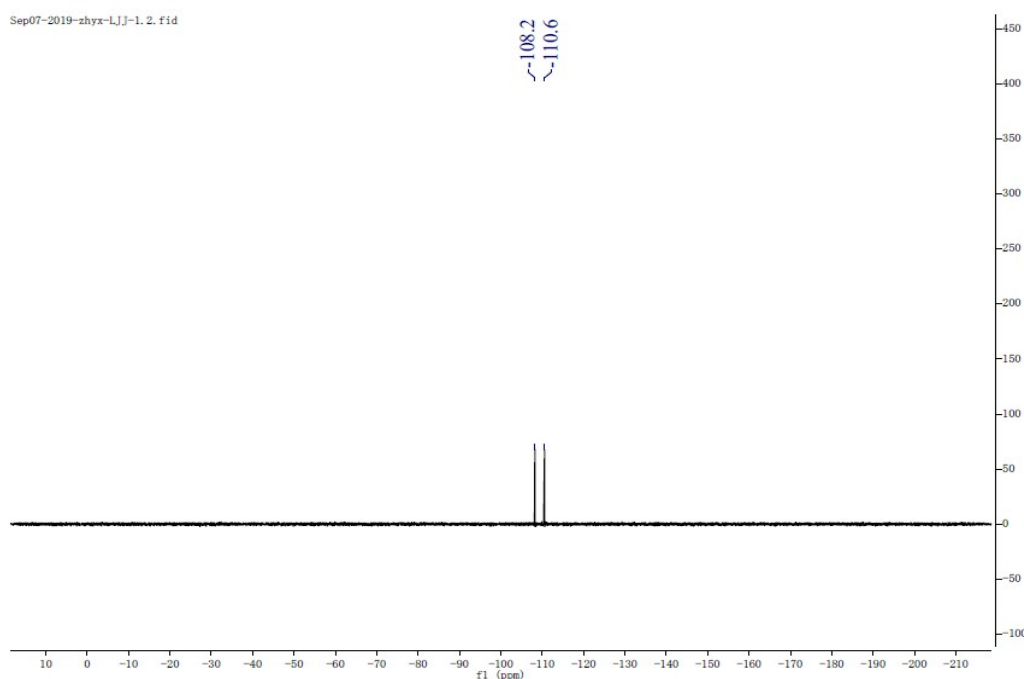


Fig. S2 The ^{13}F NMR spectrum of B-Ir1-H.

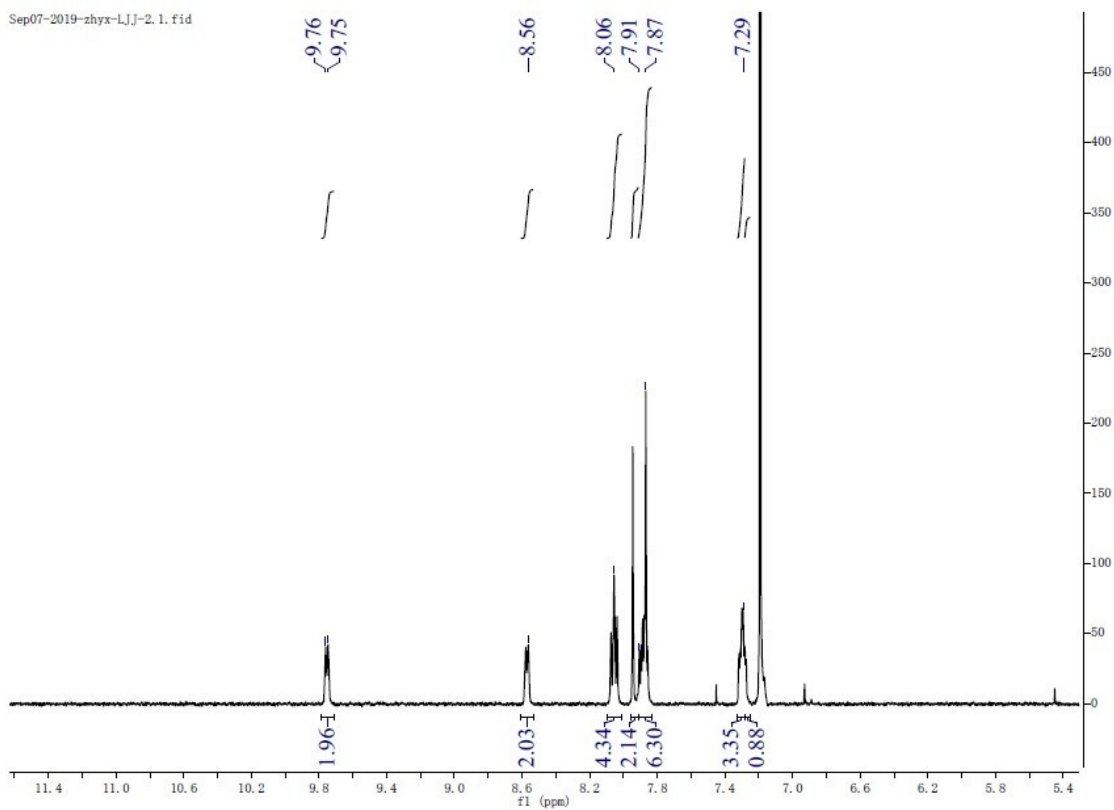


Fig. S3 The ^1H NMR spectrum of **G-Ir2-H**.

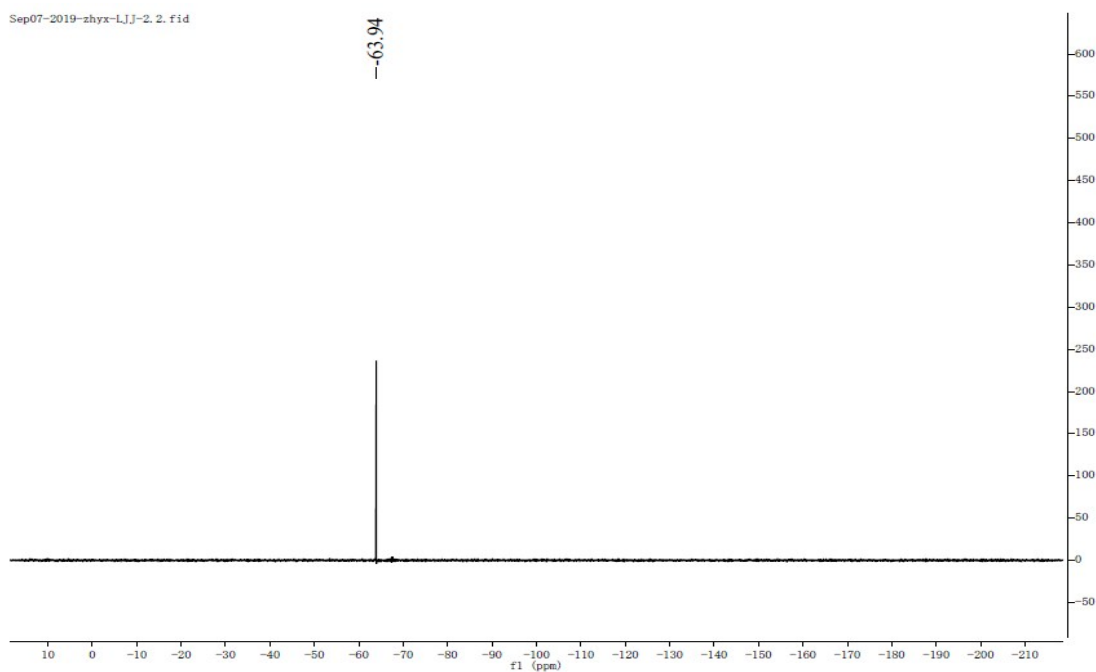


Fig. S4 The ^{13}F NMR spectrum of **G-Ir2-H**.

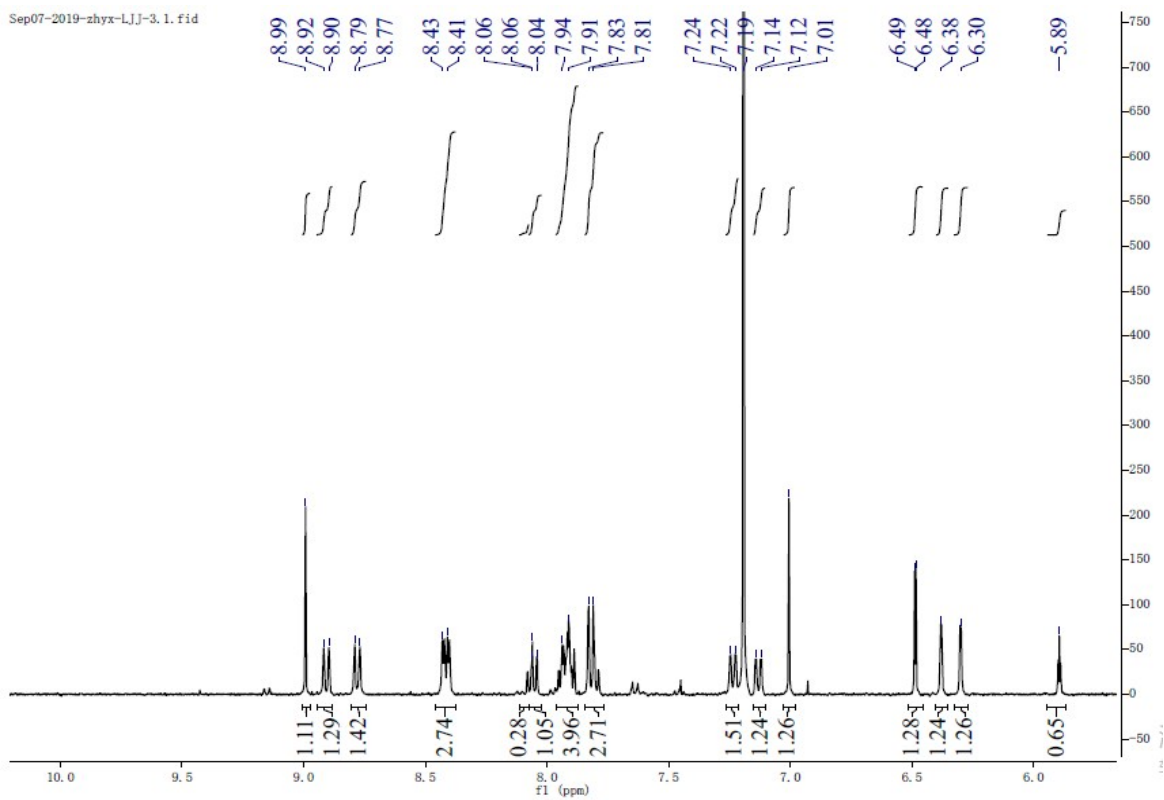


Fig. S5 The ^1H NMR spectrum of **R-Ir3-H**.

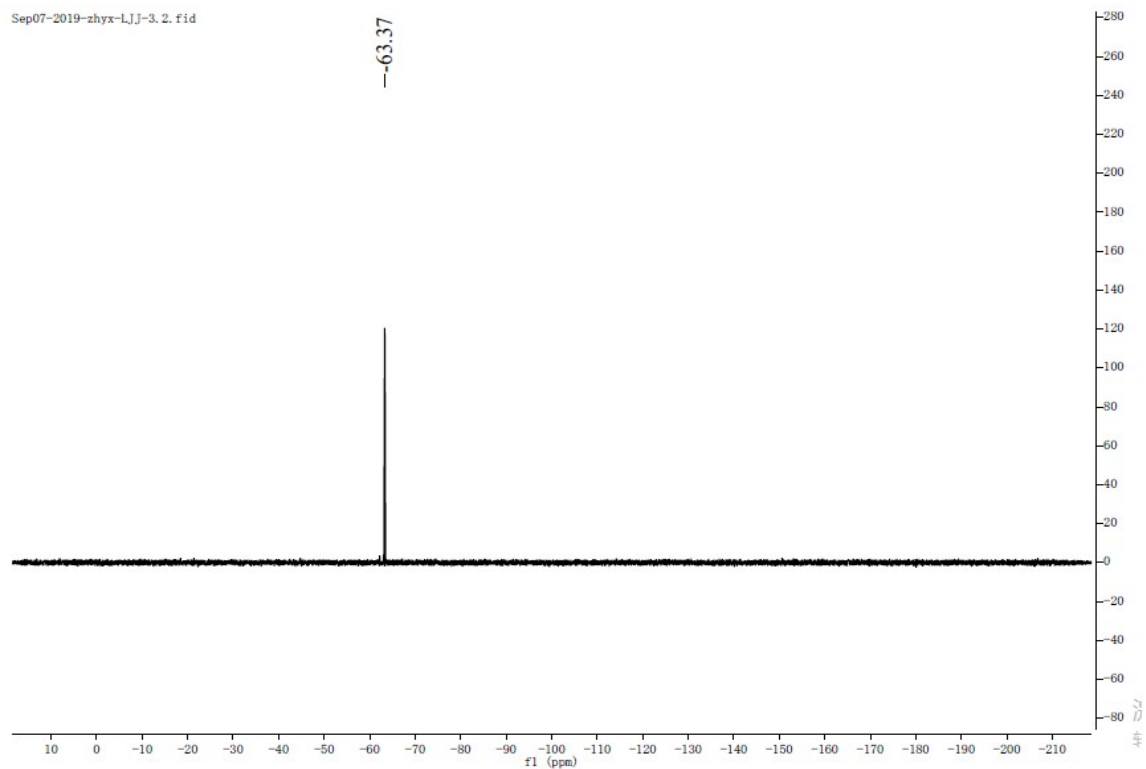


Fig. S6 The ^{13}F NMR spectrum of **R-Ir3-H**.

Mass Spectrum List Report

Analysis Info

Analysis Name D:\Data\DATA\MS-NJU\ZYX\LJJ\1911119\NJU-MS-191119001000001.d
Method DirectInfusion_TuneLow_pos.m
Sample Name Lu-01
Comment

Acquisition Date 11/19/2019 3:43:50 PM
Operator bruker
Instrument micrOTOF-Q III 8228888.20519

Acquisition Parameter

Source Type	ESI	Ion Polarity	Positive	Set Nebulizer	0.4 Bar
Focus	Active	Set Capillary	4500 V	Set Dry Heater	180 °C
Scan Begin	50 m/z	Set End Plate Offset	-500 V	Set Dry Gas	4.0 l/min
Scan End	1000 m/z	Set Collision Cell RF	540.0 Vpp	Set Divert Valve	Waste

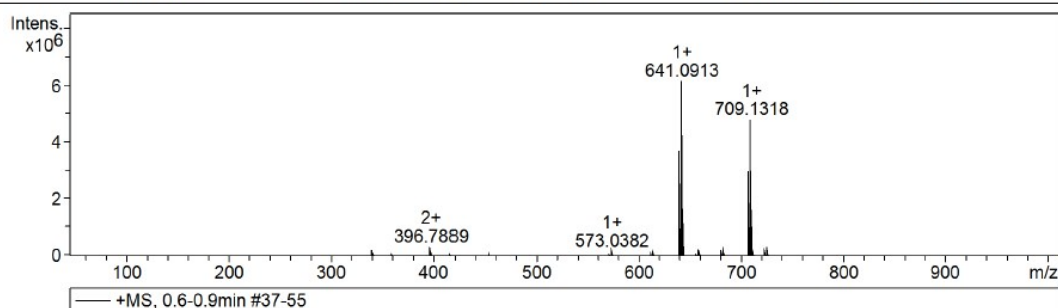
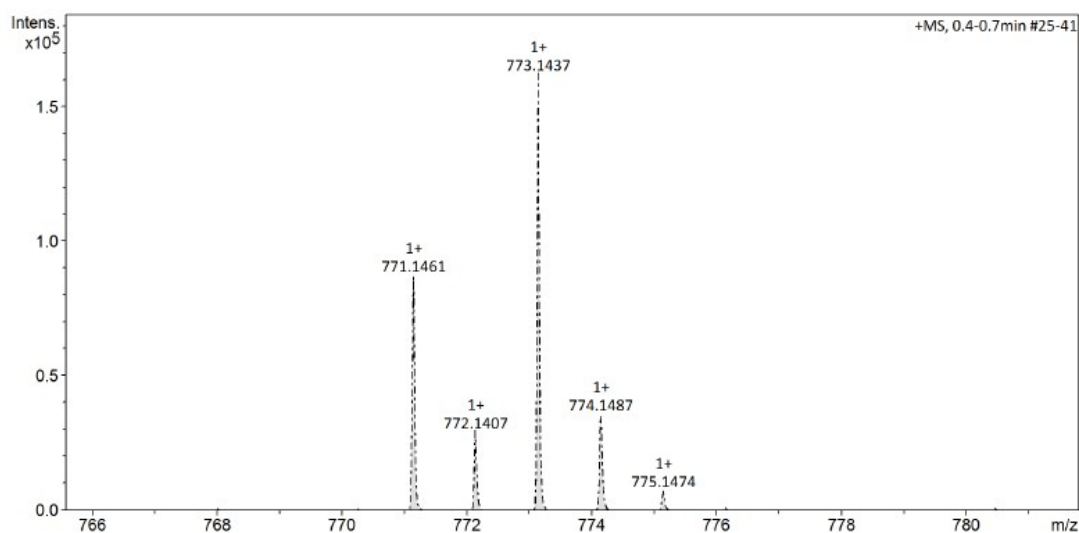
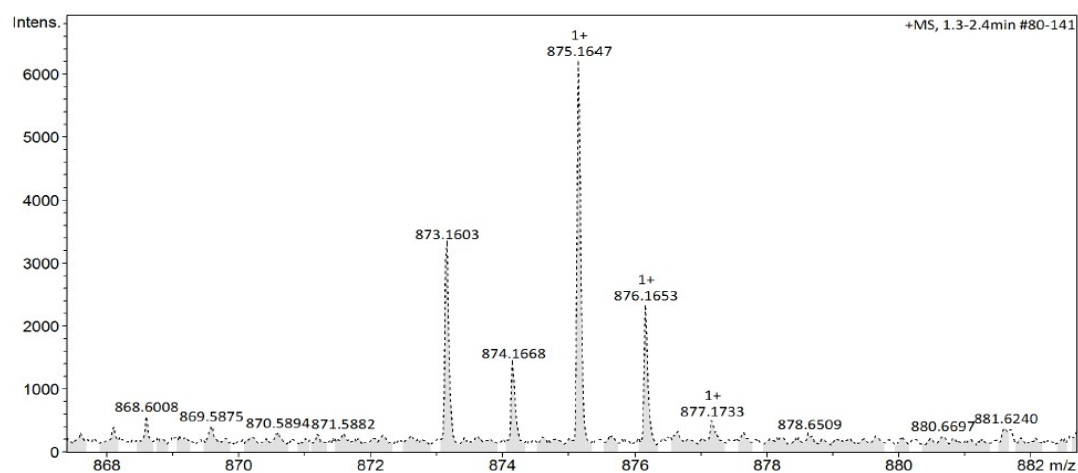


Fig. S7 The high-resolution MS spectrum of **B-Ir1-H**.



Bruker Compass DataAnalysis 4.2 printed: 11/19/2019 3:51:03 PM by: bruker Page 1 of 1

Fig. S8 The high-resolution MS spectrum of **G-Ir2-H**.



Bruker Compass DataAnalysis 4.2 printed: 11/19/2019 3:51:46 PM by: bruker Page 1 of 1

Fig. S9 The high-resolution MS spectrum of **R-Ir3-H**.

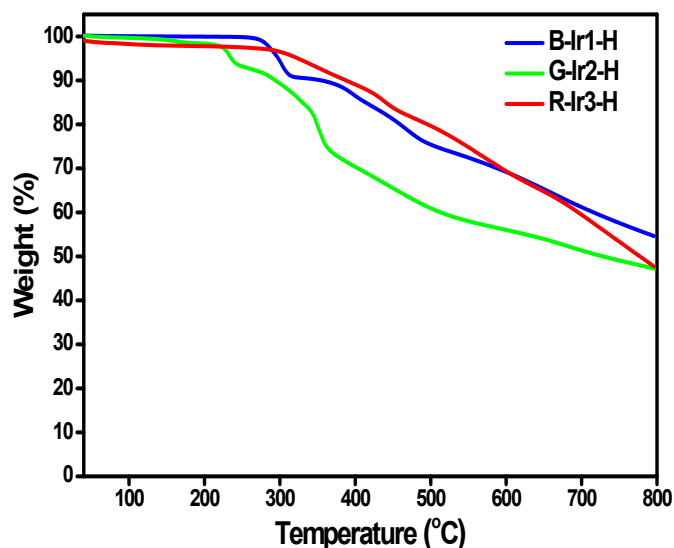


Fig. S10 TGA curves of B-Ir1-H, G-Ir2-H and R-Ir3-H.

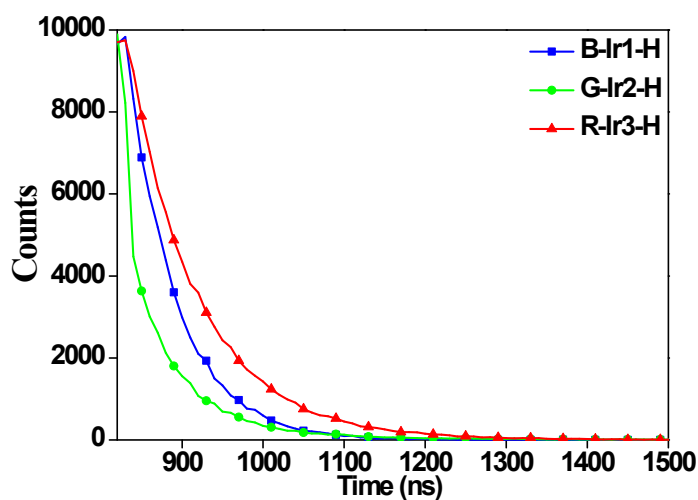


Fig. S11 The lifetime curves of B-Ir1-H, G-Ir2-H and R-Ir3-H in degassed acetonitrile solution at room temperature.

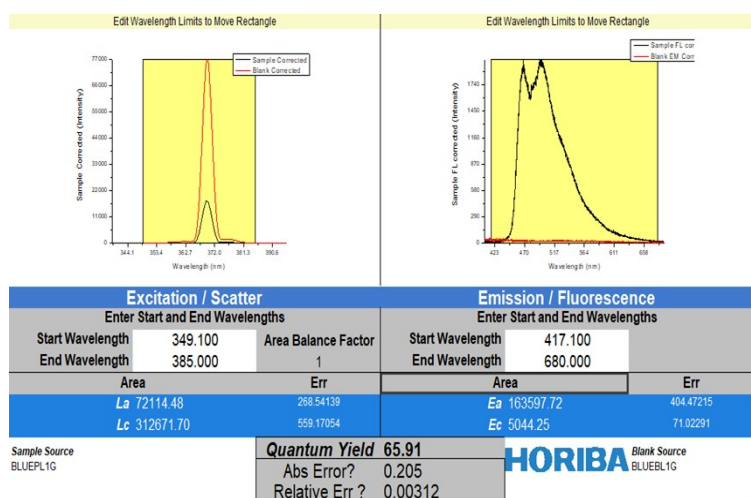


Fig. S12 The QY measurements of B-Ir1-H in degassed CH₂Cl₂ solution at room temperature.

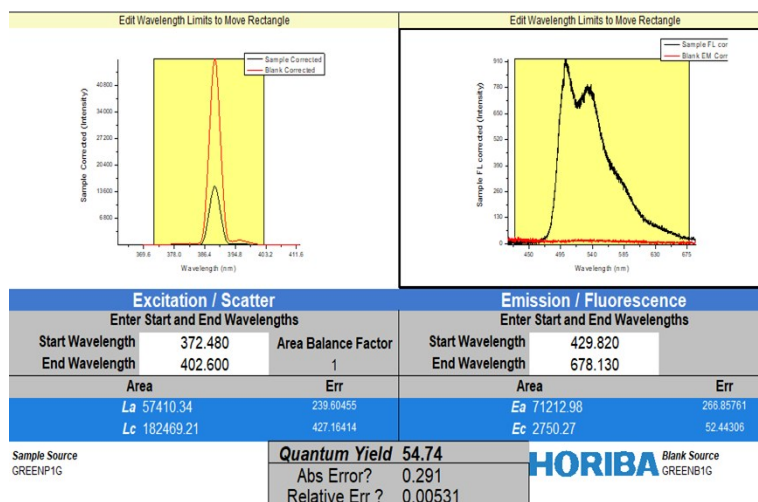


Fig. S13 The QY measurements of **G-Ir2-H** degassed CH_2Cl_2 solution at room temperature.

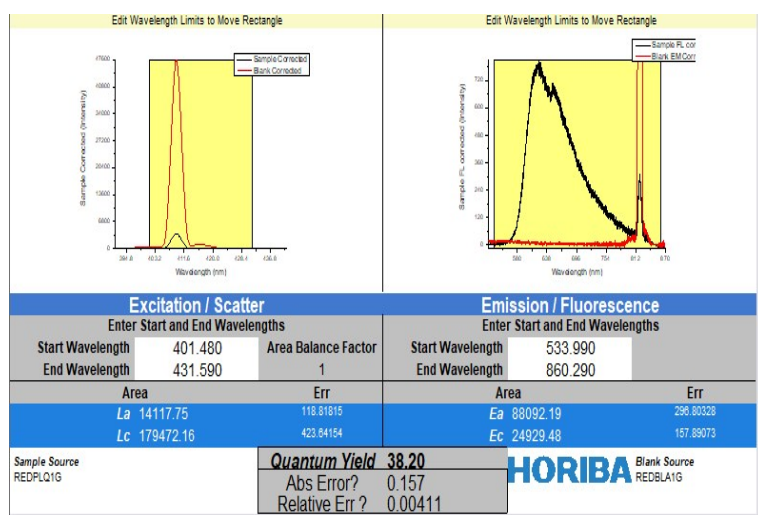


Fig. S14 The QY measurements of **R-Ir3-H** in degassed CH_2Cl_2 solution at room temperature.

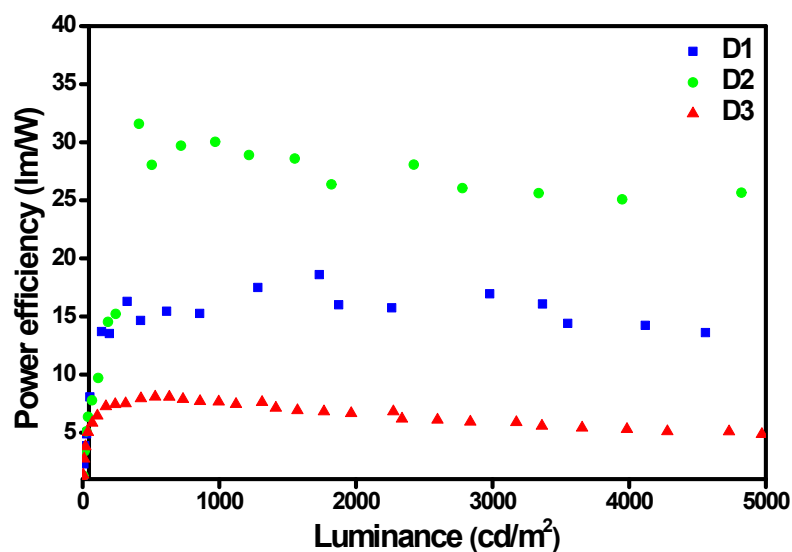


Fig. S15 Power efficiency versus luminance characteristics of the devices D1, D2 and D3.

Table S1. Crystallographic data of **B-Ir1-H**.

B-Ir1-H	
formula	C ₂₉ H ₁₈ N ₃ O ₃ F ₆ SIr
Formula weight	706.68
Temperature/K	296.15
Crystal system	monoclinic
Space group	<i>P</i> 2 ₁ / <i>n</i>
<i>a</i> (Å)	12.558(2)
<i>b</i> (Å)	13.064(2)
<i>c</i> (Å)	15.875(3)
α /°	90
β /°	102.849(3)
γ /°	90
<i>V</i> /Å ³	2539.3(7)
<i>Z</i>	4
ρ_{calc} g/cm ³	1.849
Wavelength/Å	0.71073
μ (Mo K α)/mm ⁻¹	5.318
Reflections collected with <i>I</i> > 2(<i>I</i>)	4275
Unique	9946
GOF on <i>F</i> ²	0.977
<i>R</i> ₁ ^{<i>a</i>} , <i>wR</i> ₂ ^{<i>b</i>} [<i>I</i> > 2 σ (<i>I</i>)]	0.0725, 0.0638
<i>R</i> ₁ ^{<i>a</i>} , <i>wR</i> ₂ ^{<i>b</i>} (all data)	0.0609, 0.0349

$$R_1^a = \frac{\sum ||F_o| - |F_c||}{\sum F_o}, \quad wR_2^b = \left[\frac{\sum w(F_o^2 - F_c^2)^2}{\sum w(F_o^2)} \right]^{1/2}$$

Table S2. Bond Lengths in Å for **B-Ir1-H**.

Atom	Atom	Length/Å	Atom	Atom	Length/Å
C1	C2	1.395(7)	C4	C5	1.361(7)
C1	C6	1.412(6)	C5	F2	1.366(6)
C1	Ir01	2.016(5)	C5	C6	1.387(7)
C2	C3	1.369(7)	C6	C7	1.454(7)
C3	F1	1.357(6)	C7	N3	1.366(6)
C3	C4	1.370(7)	C7	C8	1.385(7)

Atom	Atom	Length/Å	Atom	Atom	Length/Å
C8	C9	1.365(8)	C20	C21	1.370(9)
C9	C10	1.377(8)	C21	C22	1.367(7)
C10	C11	1.363(7)	C22	N4	1.351(6)
C11	N3	1.347(6)	C23	C24	1.346(8)
C12	C13	1.398(7)	C23	N2	1.348(7)
C12	C17	1.413(7)	C24	C25	1.364(8)
C12	Ir01	2.016(5)	C25	N1	1.347(6)
C13	C14	1.369(8)	C26	N6	1.331(6)
C14	C15	1.355(9)	C26	C27	1.366(8)
C14	F3	1.365(7)	C27	C28	1.345(8)
C15	C16	1.360(8)	C28	N5	1.347(6)
C16	F4	1.370(7)	Ir01	N4	2.044(4)
C16	C17	1.374(7)	Ir01	N3	2.044(4)
C17	C18	1.467(7)	Ir01	N1	2.135(4)
C18	N4	1.373(6)	Ir01	N6	2.152(4)
C18	C19	1.385(7)	N1	N2	1.361(6)
C19	C20	1.383(8)	N5	N6	1.358(5)

Table S3. Bond Angles in (°) for **B-Ir1-H**.

Atom	Atom	Atom	Angle/°	Atom	Atom	Atom	Angle/°
C2	C1	C6	119.5(4)	N3	C11	C10	122.7(5)
C2	C1	Ir01	126.9(4)	C13	C12	C17	118.1(5)
C6	C1	Ir01	113.6(3)	C13	C12	Ir01	127.1(4)
C3	C2	C1	118.4(5)	C17	C12	Ir01	114.8(3)
F1	C3	C2	118.3(5)	C14	C13	C12	118.8(6)
F1	C3	C4	117.3(5)	C15	C14	F3	117.9(6)
C2	C3	C4	124.4(5)	C15	C14	C13	124.3(6)
C5	C4	C3	115.9(5)	F3	C14	C13	117.8(7)
C4	C5	F2	115.5(5)	C14	C15	C16	116.2(6)
C4	C5	C6	124.3(5)	C15	C16	F4	116.8(6)
F2	C5	C6	120.2(5)	C15	C16	C17	123.8(6)
C5	C6	C1	117.5(5)	F4	C16	C17	119.4(5)
C5	C6	C7	126.0(5)	C16	C17	C12	118.6(5)
C1	C6	C7	116.6(4)	C16	C17	C18	126.2(5)
N3	C7	C8	119.3(5)	C12	C17	C18	115.2(5)
N3	C7	C6	112.8(4)	N4	C18	C19	119.0(5)
C8	C7	C6	127.9(5)	N4	C18	C17	113.5(5)
C9	C8	C7	120.3(5)	C19	C18	C17	127.6(5)
C8	C9	C10	120.0(6)	C20	C19	C18	120.8(6)
C11	C10	C9	118.2(6)	C21	C20	C19	119.3(6)

Atom	Atom	Atom	Angle/°
C22	C21	C20	118.9(6)
N4	C22	C21	122.7(6)
C24	C23	N2	110.5(5)
C23	C24	C25	105.6(5)
N1	C25	C24	109.5(6)
N6	C26	C27	111.3(5)
C28	C27	C26	104.9(5)
C27	C28	N5	109.4(5)
C1	Ir01	C12	88.01(19)
C1	Ir01	N4	95.50(17)
C12	Ir01	N4	80.2(2)
C1	Ir01	N3	80.24(18)
C12	Ir01	N3	96.23(19)
N4	Ir01	N3	174.57(16)
C1	Ir01	N1	90.83(17)
C12	Ir01	N1	174.05(18)
N4	Ir01	N1	94.13(17)
N3	Ir01	N1	89.32(16)
C1	Ir01	N6	174.60(16)
C12	Ir01	N6	89.61(17)
N4	Ir01	N6	88.86(15)
N3	Ir01	N6	95.22(16)
N1	Ir01	N6	92.03(16)
C25	N1	N2	107.6(4)
C25	N1	Ir01	129.2(4)
N2	N1	Ir01	122.6(3)
C23	N2	N1	106.8(5)
C11	N3	C7	119.4(4)
C11	N3	Ir01	124.0(4)
C7	N3	Ir01	116.6(3)
C22	N4	C18	119.3(5)
C22	N4	Ir01	124.2(4)
C18	N4	Ir01	116.4(3)
C28	N5	N6	108.6(4)
C26	N6	N5	105.8(4)
C26	N6	Ir01	130.1(4)
N5	N6	Ir01	124.1(3)

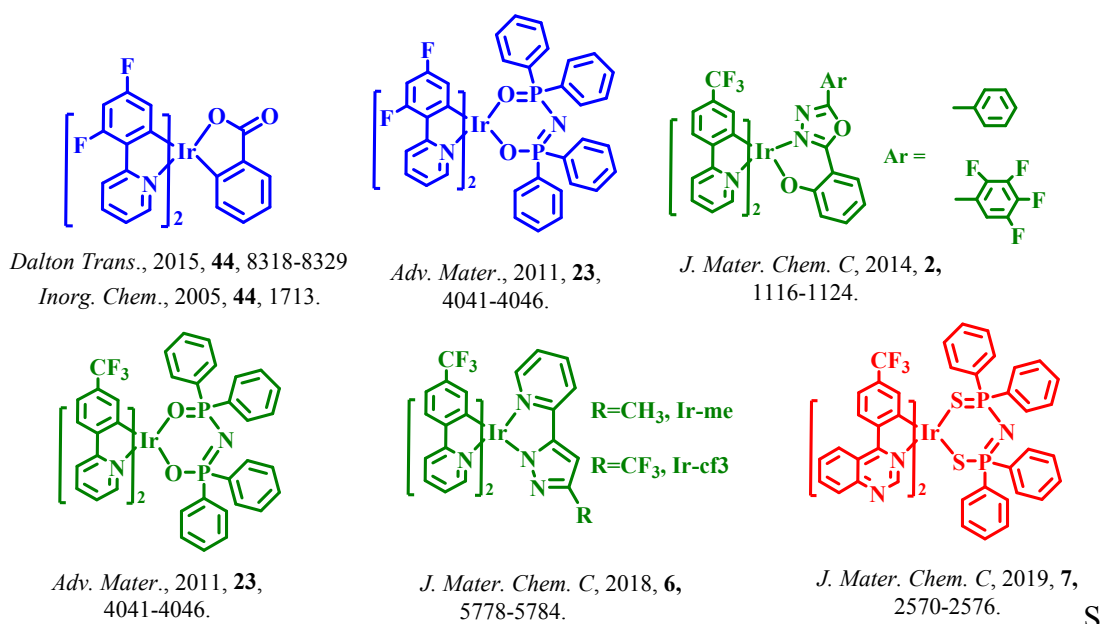
Table S4. Hydrogen Fractional Atomic Coordinates ($\times 10^4$) and Equivalent Isotropic Displacement Parameters ($\text{\AA}^2 \times 10^3$) for **B-Ir1-H_a**. U_{eq} is defined as 1/3 of the trace of the orthogonalised U_{ij} .

Atom	x	y	z	U_{eq}
H2	6261.66	2418.33	6798.66	56
H4	8783.56	4303.96	7712.74	68
H8	6500.54	6096.6	9122.3	64
H9	5168.02	6814.97	9712.24	75
H10	3400.34	6179.07	9351.79	75
H11	3044.67	4788.21	8459.4	62
H13	4003.05	5692.93	6706.8	60
H15	3409.25	5449.51	4130.3	82
H19	3668.26	1921.02	4486.87	79
H20	3805.13	214.33	4881.2	82
H21	4116.6	-218.82	6328.47	72
H22	4240.66	1049.19	7337.69	60
H23	3844.14	931.62	9790.09	72
H24	5808.27	878.02	9883.08	79
H25	6179.8	2098.74	8800.97	66
H26	1796.97	4302.85	6375.6	67
H27	23.18	3831.15	6675.37	73
H28	421.79	2619.4	7882.12	69

Table S5. The key properties (absorption maximum, emission maximum, HOMO, LUMO, etc.) of the new materials and of similar literature examples.

Complex	Absorption (λ , nm)	Emission (λ , nm)	τ (μ s)	HOMO/LUMO (eV)
B-Ir1-H	251/384	469/496	0.7	-5.80/-2.48
G-Ir2-H	254/385	492/523	0.5	-5.95/-2.96
R-Ir3-H	278/341/475	621	0.7	-5.94/-3.45

FIrpic	250/350/440	468/495/535	1.4	-5.8/-2.90
Ir(dfppy)₂(tpip)	240/388/443	485/515	0.77	-5.51/-2.87
Ir(tfmpppy)₂(tpip)	350/412//464	524/560	0.89	-5.44/-2.98
Ir1	261/406	524/566	2.31	-5.38/-2.61
Ir3	255/413	520/556	2.03	-5.38/-2.75
Ir-me	267/390/450	499/523	1.92	-5.55/-3.07
Ir-cf3	267/385/449	494/523	2.34	-5.78/-3.30
Ir(tfpqz)₂	285/348/435/486	624	1.94	-5.72/-3.72



cheme S1. The molecular structures of some example materials and their references.

References:

1. *SAINT-Plus, version 6.02*, Bruker Analytical X-ray System, Madison, WI, 1999.
2. G. M. Sheldrick, *SADABS An empirical absorption correction program, Bruker Analytical X-ray Systems, Madison, WI, 1996.*
3. G. M. Sheldrick, *SHELXTL-2014*, Universität of Göttingen, Göttingen, Germany, 2014.